Carbon nanofibers as catalyst support

—

Developing an H_2-based recipe for plasma enhanced chemical vapor deposition.

John Schack

Degree Project in Materials Chemistry, 2024
Center for Analysis and Synthesis
Lund University
Sweden

30 ECTS credits

LUND
UNIVERSITY

Populärvetenskaplig sammanfattning

Det här projektet har handlat om att utveckla ett sett att använda vätgas i ”receptet” för att tillverka kolnanofibrer. Dessa kan sedan användas för att effektivisera framställningen av grön vätgas. Grön vätgas är centralt när det kommer till hållbar omställning inom flera olika industrier. De stora satsningarna på grönt stål i Sverige är till exempel beroende av grön vätgas, likaså behövs den gröna vätgasen inom områden som bränsle för långväga transporter, hållbart konstgödsel med flera.

En lovande metod för att tillverka grön vätgas är protonutbytesmembran-elektrolys, denna metod står inför en stor utmaning då den sällsynta metallen iridium är central i tekniken. Den är så pass sällsynt att utan mer effektiv användning kommer dagens fyndigheter inte att räcka till. Här kan kolnanofibrerna komma till nytta. Samma mängd vätgas kan produceras med en mindre mängd iridium genom att placera metallen på en nanostruktur som ökar kontakten med nästa lager i elektrolysören.

Vad är en kolnanofiber då? Tanken går lätt till kolfibrer som används i många lättviktsmaterial, till exempel sport-cyklar. Skillnaden är att kolnanofibrer är betydligt mindre och består av en mer ordnad struktur. Kolatomerna som bygger upp fibrerna binder alla till tre grannar och bildar lager av kol - ett sådant isolerat lager är vad som kallas grafen, ett material som fått mycket uppmärksamhet för sina unika egenskaper. I en kolnanofiber är flera lager i stället ordnade som, till exempel, många i varandra staplade koner eller flera ihoprullade lager. Dessa fibrer är ofta några tiotals nanometer i diameter och några mikrometer långa. Som jämförelse är de ca 50 000 gånger smalare än ett hårstrå.

För att få kolnanofibrer att växa används ofta en process med två gaser, en kolbärande gas och en gas vars syfte är att hindra konkurrerande processer genom att etsa bort mindre välordnade kolstrukturer - denna roll fyller typiskt ammoniak och mitt projekt har handlat om att visa att användning av vätgas kan vara ett alternativ. Detta är intressant då nya sätt att kontrollera processen, till exempel hur tätt fibrerna växer, kan upptäckas och vara användbara för applikationen i elektrolys. Vätgas kan också vara trevligare att arbeta med än ammoniak.

I projektet har jag visat att det här bytet är möjligt, med ett tydligt återstående problem: längden på fibrerna. Bilder från elektronmikroskop har visat hur en fiber ser ut i detalj vilket ger ökad förståelse för processen. Receptet innehåller en lång lista på ingredienser och resultaten har gett uppslag kring vilka av dem som behöver balanseras ytterligare för att få växthastigheten att skjuta i höjden.

Abstract

This study investigated growth of carbon nanofibers (CNF) using hydrogen (H_2) gas on a porous titanium substrate. The target is uniform coverage of vertically aligned CNFs on the substrate, with length of a few micrometers, to produce a surface area enhancement – the intended application of this structure is as a catalyst support. CNFs were synthesized in a plasma enhanced chemical vapor deposition (PECVD) reactor using acetylene (C_2H_2) and H_2. The impact of the gas ratio and temperature was studied for two catalysts, Ni and Fe. Initially, vertically aligned CNF growth using the Fe catalyst was observed with high density of CNFs ($1.6 \cdot 10^{10}$ fibers/cm^2), average length of around 146 nm and uniform coverage over the substrate after a 15 minute growth process. However, later the reproducibility came into question with the observation of a different growth regime, distinguished by the presence of film growth on the samples and significantly lower density. A few observations possibly related to the governing dynamics behind these two growth regimes are discussed.

The CNF morphology was elucidated, and it was found that the fibers grown appear to have a core-shell Fe/carbon nanotube (CNT) morphology with an elongated catalyst particle core. The Ni-catalyzed growth was unsuccessful while Fe-catalyzed growth shows promise, with some remaining issues regarding reproducibility and growth rate. This study has provided a basis to suggest a few reasonable routes towards improving these issues. These include studying the plasma parameters and the catalyst particle adhesion to the substrate.

Preface/Acknowledgements

This thesis was done during spring/winter of 2024 in collaboration with Smoltek Hydrogen AB, a company based in Gothenburg that takes aim at developing the next generation of proton exchange membrane water electrolyzers. The key to this development is to leverage the use of carbon nanostructures, specifically carbon nanofibers to increase the utilization of the catalyst and to enable application of a thin catalyst layer while maintaining long-term durability. My project has involved development of a new growth recipe for the carbon nanofibers, with the aim of replacing ammonia with hydrogen gas in the process.

During my work on this thesis, I have received invaluable guidance and support from both my supervisors, Shafiq Kabir at Smoltek, and Martin Ek Rosén at Lund University. Also, I want to especially thank Bastien Penninckx who instructed me on how to use the PECVD reactor, prepare samples, aided with catalyst deposition, and answered all my questions. A special thanks also to Xin Wen for help with TEM sample preparation and image analysis and to Elin Grånäs, Amin Saleem and Qi Li for many helpful discussions. To my manager Fabian, thanks for your support and for helpful discussions and advice about my future career. To Réka Simon-Balint, Ellinor Ehrnberg, Sankar Sasidarhan thanks for your patience in explaining about everything else at Smoltek Hydrogen, the project planning and safety work; the market and investor perspectives and the intricate details of the electrolysis process. And to Edit Helgee and Louise Duker thanks for sharing your knowledge about patents and business development in our group meetings. Finally, my gratitude to everyone else at Smoltek for making me feel welcome during my time at the company.

Contents

List of abbreviations

PEM – Proton Exchange Membrane

PTL – Porous Transport Layer

CNF – Carbon Nanofiber

PECVD – Plasma-enhanced Chemical Vapor Deposition

CNT – Carbon Nanotube

CVD – Chemical Vapor Deposition

PVD – Physical Vapor Deposition

SEM – Scanning Electron Microscope

TEM – Transmission Electron Microscope

EDX(S) – Energy Dispersive X-ray Spectroscopy

DC-PECVD – Direct Current Plasma Enhanced Chemical Vapor Deposition

VLS – Vapor-Liquid-Solid

VSS – Vapor-Solid-Solid

HRTEM – High Resolution Transmission Electron Microscopy

STEM – Scanning Transmission Electron Microscopy

FFT – Fast Fourier Transform

1 Introduction

For many emerging technologies in the transition towards a climate neutral industry, green hydrogen is central. This is true for the production of green steel, sustainable fuels for shipping (e.g. hydrogen gas or ammonia), hydrogen fuel cell technology, energy storage applications etc. Proton exchange membrane (PEM) electrolyzers are one of the more promising methods to produce green hydrogen. A key advantage is the possibility of producing green hydrogen from intermittent power sources, such as wind and solar. Kojima et al. discuss this in a 2023 review where they highlight the advantage of PEM electrolyzers in terms of operability at low power load and with fluctuating power, while also stressing the need to develop solutions for more efficient catalyst utilization [1]

The catalyst is needed for the oxygen evolution reaction (OER), where water is split into oxygen and hydrogen ions/protons. The current state of the art catalyst is iridium or iridium oxide, which strikes a balance between activity and stability in the harsh oxidative conditions of the cell [2]. Reducing the amount of iridium needed while maintaining efficiency and current density of the cell is a key area of development for the technology as price and availability of iridium limits its potential[2][3]. To do this carbon nanofibers (CNFs) can be used as a high surface area catalyst support with high utilization of the catalyst and good durability at low loading compared to the traditional catalyst ink solutions.

The CNFs are grown on top of a porous titanium substrate. The substrate is a part of an electrolysis cell called a porous transport layer (PTL). The PTL allow transport of water to the catalyst, conduction of electrons to supply the OER and transport of oxygen gas. Vertically aligned CNFs, suitable for this application, are typically produced using plasma enhanced chemical vapor deposition (PECVD) with acetylene (C_2H_2) as a carbon precursor and ammonia (NH_3) as an etchant gas. For the etchant gas there is also the option of using hydrogen gas (H_2). The use of H_2 for PECVD growth of CNFs is not well studied and there is a gap both in terms of systematic parametric studies of this process in general and specifically for growth on a porous titanium substrate. One challenge faced in studying this is the complexity that comes with a large parameter space for the growth process. Each reactor system provides slightly different conditions which affects the resulting growth. With this in mind, each study provides new information that can be an added piece of the puzzle when designing future experiments.

This project aims to contribute by investigating the H_2 growth process of vertically aligned CNFs on a porous titanium substrate. The goals are twofold: optimizing growth parameters to produce CNFs with morphology suitable for use as catalyst support while demonstrating the feasibility of H_2 as etchant gas in this process; and to increase understanding of the growth mechanism.

Apart from better understanding of the growth process, a motivation for developing recipes using H_2 is to eliminate some of the risks associated with the use of NH_3. With nitrogen present there could be residual hydrogen cyanide (HCN) from the process. The presence of HCN in the residual gas mixture has been reported previously[5]. The exposure to HCN and NH_3 is regulated through occupational exposure limits issued by the Swedish Work Environment Authority (AFS 2018:1).

The administrative load of considering the consequences of working with these toxic and polluting substances can be relieved by excluding NH_3 from the process. Additionally, it can be argued to be a more sustainable choice due to the circularity created when using the electrolysis product, H_2, as input to the electrolysis cell production.

The experimental part of the project was conducted in two phases where the first phase had the goal of producing the desired CNF morphology by exploring the impact of the gas ratio, temperature and catalyst material. The second phase consisted of trials to extend the growth time and study the temperature dependency – with potential to investigate the activation energy for the growth process and linking the results to the growth mechanism. The experiments were performed in the MC2 clean room lab at Chalmers University. PTL substrates with growth catalysts deposited on top were prepared using physical vapor deposition (PVD). The CNF growth was done in Smolteks proprietary PECVD equipment and characterization by using scanning electron microscopy (SEM), transmission electron microscopy (TEM) and energy dispersive x-ray spectroscopy (EDX(S)).

2 Background

This section aims to provide theoretical background and context for the experiments done in this project. CNFs is a broad category of fiber-like carbon nanostructures with a diverse range of synthesis methods. Two categories are often highlighted, catalytic chemical vapor deposition (CVD) and electrospinning methods [6]. There are many variants of CVD methods used to grow CNFs; for synthesis of free-standing vertically aligned CNFs, PECVD is often used. The typical electrospinning process uses polyacrylonitrile to form polymer fibers which are post-processed into CNFs. Potential or current applications are found in areas such as catalytic support, fuel cell systems, hydrogen storage devices, reinforced polymer materials, electromagnetic microwave absorption [7], CO_2 capture, battery and supercapacitor technology as well as several biomedical applications [6]. It is fair to say that CNFs/CNTs show great promise as part of future solutions to important challenges facing our society.

In the rest of this section the focus is on PECVD grown fibers since this is the method used in this project. The section includes an introduction to the PECVD process, the catalyst deposition process, an overview of the research on CNFs, and a discussion surrounding the multitude of parameters that can influence the growth process.

2.1 Carbon nanofibers

Carbon fibers, or filaments, have been studied since at least the late 19$^{\text{th}}$ century [8]. The study and understanding of CNFs started later with the invention of electron microscopy and other methods allowing observation at the nanoscale. The interest in the field took off after the synthesis and characterization by TEM of "helical microtubules of graphitic carbon" was performed by Iijima in 1991, later named carbon nanotubes (CNT) [9]. Since then, there have been many proposed applications for CNFs and CNTs, as mentioned above. CNFs grown by

PECVD are formed from layers of graphitic carbon, they can be classified into three categories depending on the angle between the layers and the growth direction [7], illustrated in Figure 1. There are also many variations from these structures, see e.g. table 2 and 3 in [7]. The CNF term is often used as an umbrella term referring to all kinds of carbonaceous nanofiber growth while some literature makes a distinction by referring to cases a) and b) in figure 1 as CNTs, with a) being a special case, and only other morphologies like in c) and d) are referred to as CNFs.

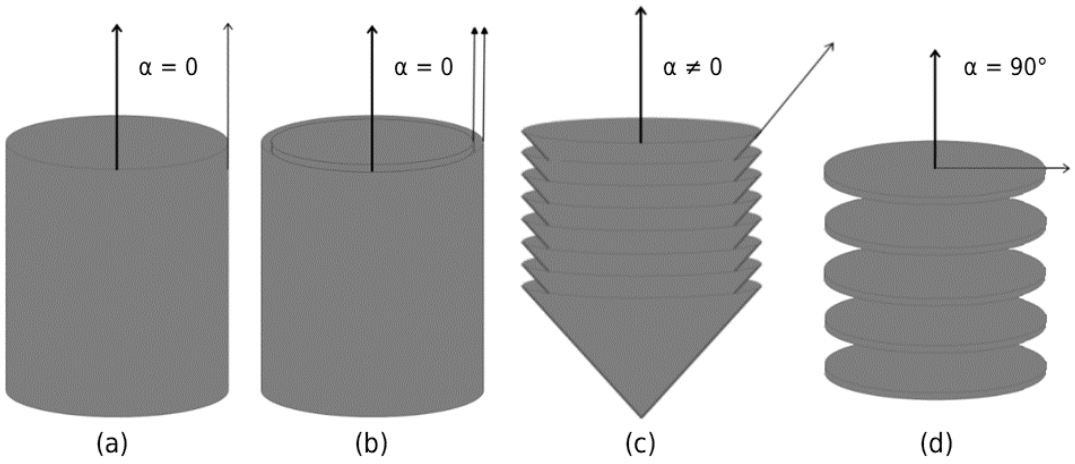

Figure 1: a) Single-walled CNT. b) Multi-walled CNT/CNF. c) Cone or herringbone/fishbone CNF. d) Platelet CNF. Figure adapted with permission from [10].

In this thesis I mostly use CNF in the umbrella term capacity and CNT when citing another study using this term or when discussing the structure in detail.

In PECVD CNFs are grown using a catalyst particle, e.g. Ni, Fe, Co, Pd. A balance between carbon supply and etching is needed to grow CNFs, this and other details about PECVD growth is expanded upon in section 2.2. If the carbon supply is too low the deposition cannot keep up with the etching so no growth can happen. In the opposite scenario, when carbon supply is too high there is buildup of amorphous or poor quality carbon, according to Chhowalla et al, who also suggested insufficient etching can cause deactivation of the catalyst particle due to the surface being covered with carbon [11].

An important aspect of catalytic CNF growth is the growth mode. There are two types commonly discussed in literature: base type and tip type. For base-type growth the catalyst particle stays at the substrate while the CNF grows on top. For tip-type growth the catalyst particle stays on top of the growing CNF. The two growth modes are illustrated schematically in Figure 2.

The growth mode is an important factor in controlling the vertical alignment of the CNFs often seen in PECVD growth. It has been suggested that the electric field between the electrodes (see Figure 3) induces stress at the catalyst/nanofiber interface. For tip-type growth these stresses create negative feedback when a CNF starts to bend, i.e. when the growth rate on one side starts to exceed the one on the other side this feedback mechanism reduces the growth rate for the faster growing side. This keeps the growth rate uniform for the different sides of the CNF, leading

to vertically aligned growth. For base-type growth the feedback is instead positive and aligned growth is unfavored [12].

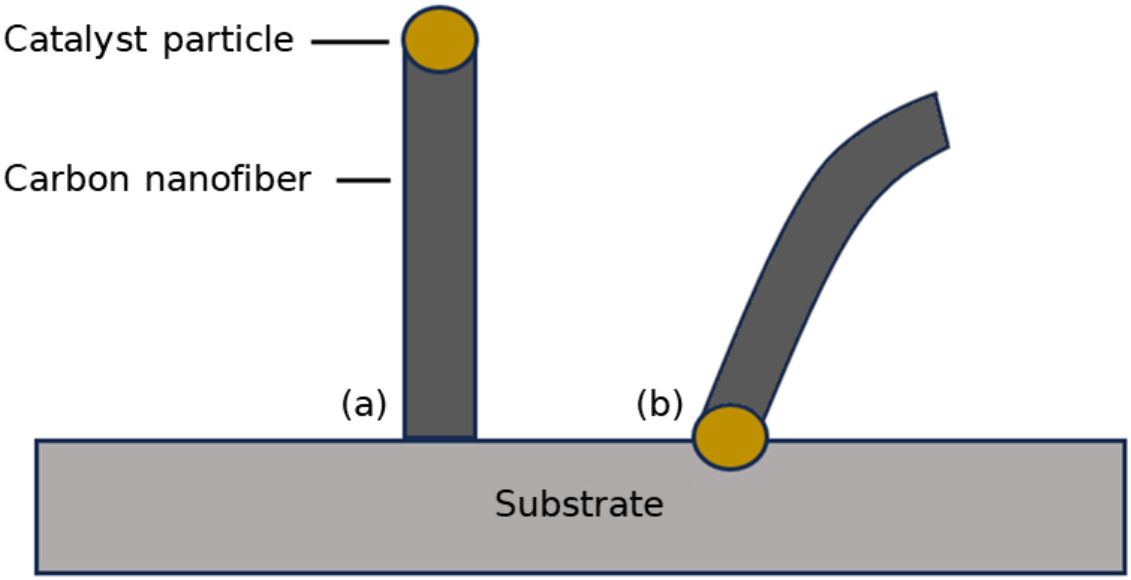

Figure 2: Schematic illustration of a) tip-type growth; and b) base-type growth of CNFs in PECVD.

Many suggestions have been put forward for what governs the growth mode. One suggestion is that the bombardment of ions in PECVD might favor tip-type growth due to loosening of the catalyst particle from the substrate [13]. Another study consider the temperature gradient in the catalyst particle and propose that this gradient, which can be induced by difference in heating from the plasma and the substrate heating plate, determines base or tip type growth [14]. A third proposal is that the ratio between the carbon source gas and the etchant gas is important. If the ratio is low, etchant species from the plasma will keep the catalyst surface clean. On the clean surface, carbon can diffuse from the top and precipitate at the bottom of the catalyst – thus leading to tip type growth. If the ratio is high an amorphous cap will form and cover the catalyst particle. In this case carbon can only diffuse in from the side via the substrate. A concentration gradient forms leading to diffusion upwards and precipitation of carbon to grow the CNF on top of the catalyst particle, i.e. base-type growth [15].

One topic of debate surrounding CNF growth is by which mechanism the CNF grows. The commonly used catalyst Ni was studied already in 1972 by Baker et al., they performed growth of filamentous carbon from decomposition of acetylene. They postulate a vapor-liquid-solid (VLS) mechanism and support this by noting that the activation energy for the growth process is very close to that of C diffusion through a liquid Ni catalyst [16].

Later studies, using PECVD, demonstrated CNF growth at lower temperatures and the VLS mechanism was challenged. In 2002 Ducati et al. argue that the growth occurs via a vapor-solid-solid (VSS) mechanism. Deposited carbon diffuses through the catalyst particle, forming a solid solution that, when saturated, precipitates to grow CNTs. They study the growth in the

temperature range 550 °C to 900 °C. In 2003, Hofmann et al presented the growth of CNFs at temperatures ranging from as low as 120 °C to 530 °C and argue that surface diffusion explains the low temperature growth using Ni [17]. Ni is the most well studied catalyst and large parametric studies have been done, e.g. by Chhowalla et al. on the Ni-catalyzed growth [11].

For Fe-catalyzed growth the analysis becomes more complex due to the possibility of different phases being active during growth. Yoshida et al showed in 2008 that the Fe catalyst particle in CVD growth of base-type CNTs is an iron carbide, Fe_3C [18]. It was later showed by Wirth et al. in 2012 that α-Fe, ɣ-Fe and Fe_3C can be the active catalyst in this process [19]. According to their paper the carbide forms during annealing from α-Fe particles but not ɣ-Fe. They go on to argue that the presence of α-Fe or ɣ-Fe is governed by the amount of carbon contaminations in the chamber during annealing. In 2011 He et al. investigated Fe catalysts using direct current PECVD (DC-PECVD) growth of tip-type, vertically aligned CNFs and find that for growth at 600 °C only Fe_3C is present whilst at higher temperatures (650, 725 °C) there is a mix of α-Fe and Fe_3C. They show that the growth rate is higher for α-Fe-catalyzed CNFs and attribute this to surface diffusion of carbon in α-Fe and bulk diffusion in Fe_3C together with the accompanying difference in diffusion rates. Based on high resolution transmission electron microscopy (HRTEM) images they argue that graphite is nucleated from step-edges on the catalyst particles, for both α-Fe and Fe_3C. In their study they deposit 10 nm Fe films [20]. They compare the mechanism for Fe with that for Ni-catalyzed growth, studied by the Hofmann group mentioned above. A study by Cantoro et al. find that the thickness of Fe films and the use of DC plasma can influence whether the grown structures are dense forests of thin CNTs or more sparsely distributed, wider diameter, CNFs. They find that using DC PECVD with Fe films thicker than 5 nm yields nucleation of CNFs, at temperatures around 500-550 °C [21].

2.2 The PECVD process and catalyst deposition

PECVD is a common method of synthesizing CNFs, it is especially useful for achieving sparse density, vertically aligned CNFs. Typically, in DC-PECVD a carbon precursor gas (e.g. CH_4, C_2H_2) and an etchant gas (e.g. NH_3, H_2) are introduced into a growth chamber where the growth substrate is placed on a heated bottom electrode. For PECVD there are also many categories, e.g. microwave plasma CVD, inductively coupled plasma CVD, radio frequency plasma CVD etc. This background is limited to the DC-PECVD method used in this project.

A schematic view of the PECVD reactor used in this project is shown in Figure 3. The interlayer is optional in the process but is often used to avoid interdiffusion and alloying of the substrate and the catalyst layer, e.g. formation of silicides when using a Si substrate [22].

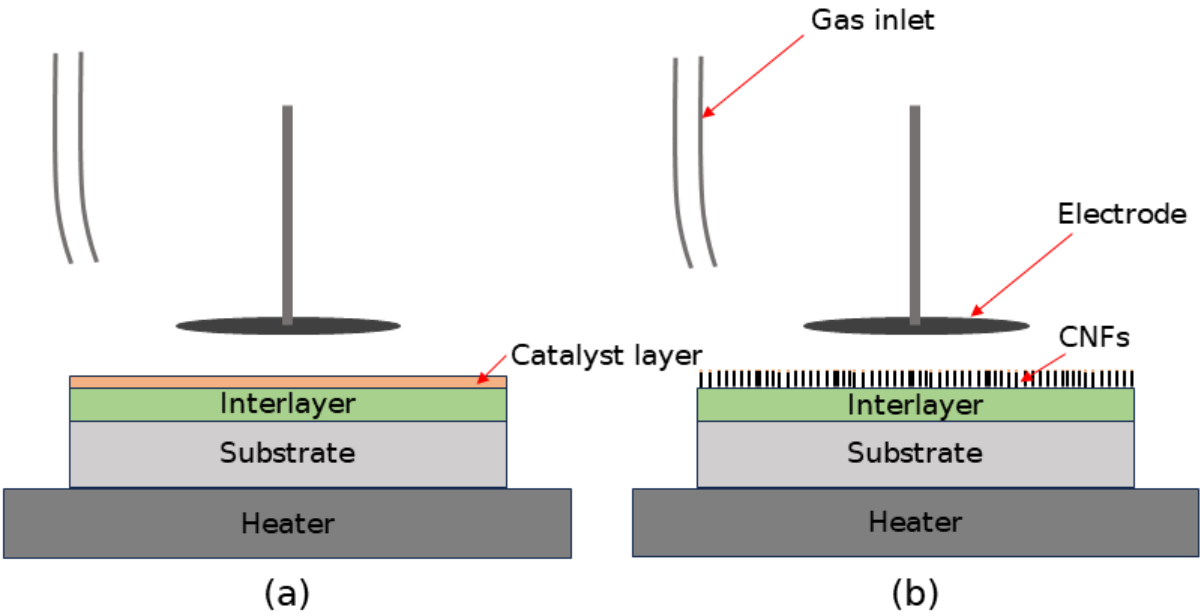

Figure 3: Schematic illustrations of the PECVD reactor. The interlayer is optional and typically used as an anti-diffusion layer. The heater and substrate acts as bottom electrode a) Before heating. b) After heating and CNF growth. Not to scale.

In DC-PECVD the reaction chamber is first heated and when at growth temperature the gas inlet is opened and a DC voltage is applied, or sometimes a pulsed DC voltage is used – typically with a frequency of around 5-100 kHz. Once the plasma has been ignited it serves two general purposes: The heat and ion bombardment increases dissociation of the carbon precursor and ions, especially hydrogen ions from the etchant gas, are accelerated towards the substrate, etching amorphous carbon that forms on the catalyst particle surfaces [17]. The plasma process is complex and to achieve CNF growth the balance between the etching properties and the carbon supply is key. This balance is regulated primarily by the ratio of carbon precursor gas to etchant gas but it is also part of an intricate interplay with other parameters, e.g. heat, plasma power etc. which is exemplified in Chhowalla et al. [11].

Growth of CNFs is a complex process, as evidenced by the difficulty of reproducing experiments [23], [24]. Even before the experimental parameters for growth in the PECVD reactor are considered there are many choices: The substrate, use of interlayer, choice of catalyst and thickness of deposited layers. For each application there are different requirements when it comes to these choices. Consequently, it is difficult to find previous studies with conditions matching your own requirements.

For the growth process there are some key parameters to consider: gas ratio, temperature, pressure, gas flow, working distance (distance between top electrode and bottom electrode/substrate, plasma power, voltage, and frequency. Vollebregt et al. also discuss hidden parameters such as reactor geometry and humidity in the lab, which are rarely presented in publications [23].

The role of the catalyst is to provide nucleation points for the carbon dissociation/adsorption and the catalyst should also allow diffusion of carbon so that the adsorbed carbon can be

incorporated into the growing nanofiber. The catalyst is often deposited as a film, this can be done by many methods, e.g. e-beam evaporation [25], electroplating [26] and sputtering [27]. From the film, particles can form under heating in a process called dewetting. This is explained simply in Randolph et al. as minimization of interfacial energy when the thin film separates into particles or "islands" [27]. Delving deep into this topic is outside the scope of this thesis but it is important to mention since it adds complexity to the process. It has been shown that the conditions of the film deposition can influence the dewetting and, consequently, the growth results [27]. Some studies also deposit particles directly, e.g. by patterning the sample [24] or using spark ablation printing [28].

In conclusion, the parameter space for this process is huge which leads to necessary limitations in the experimental scope. If all important parameters are studied the number of experiments easily runs in the hundreds. The parameters targeted in the experiments done as part of this thesis project were decided after an extensive literature review and based on their influence on the growth of CNFs as well as some practical considerations which will be discussed in the experimental method section below.

3 Setting up phase one: the parameter search

In the literature, cases of vertically aligned CNFs grown by PECVD using H_2 are rare. H_2 is often found among the process gases in thermal CVD of carbon nanotubes, but it appears that NH_3 is preferred for PECVD. With regards to plasma chemistry, one study by Woo et al. suggests that H-ions are the most important etchant species and go on to claim that these are generated more efficiently in an NH_3 plasma compared to H_2 [29]. A plausible conclusion from this is that one might expect the optimal C_2H_2:H_2 ratio to be higher in etchant gas than with a NH_3-based process.

One group from TU Delft have published several papers using C_2H_2 and H_2. In one study from early 2022 they test ratios in the range 1:28 to 1:140 and find the highest density of fibers at a ratio of 1:35, growing CNFs using a Ni catalyst in a pulsed DC-PECVD system [30]. In another paper later the same year they use this ratio of 1:35 in trials using spark ablation deposited catalyst [28]. In contrast to this, Tabatabaei et al. grow vertically aligned CNFs using a special AC-DC PECVD set up and a ratio of C_2H_2 to H_2 of 1:2 [31]. Morjan et al. use a 1 nm Fe catalyst film and find growth of dense forest of CNTs using DC-PECVD and a C_2H_2:H_2 ratio of 1:3, at a temperature of 700 °C.

Based on the literature review the gas flow ratio and the catalyst are important parameters for CNF growth and these are the main parameters targeted here. Additionally, the temperature is included as a variable, due to its influence on the growth rate. Also, the results at different temperatures might give helpful indications when preparing for the second phase where study of the CNF growth over a wider range of temperatures and growth time is planned.

In this phase, two catalysts are explored: Ni and Fe. The selection was based on the literature review, previous experience at Smoltek and availability in the lab. Both catalysts were deposited as thin films with a thickness of 9 nm. For Ni there are previous studies at TU Delft achieving an interesting morphology (see figure 4b in [30]) using a 9 nm film. Many studies use Fe as catalyst for specifically thin CNT growth but findings in Cantoro et al. suggest that nucleation of thicker CNFs is possible using >5 nm Fe films [21]. Other catalysts like Co and Pd are used in literature but not considered here due to time constraints.

4 Experimental method

The experiments were performed in Smolteks proprietary PECVD reactor, equipped with a DC power supply unit for the plasma and a heater capable of heating the substrate to a maximum temperature of 590 °C. There was no computer interface available for the system meaning no automatic data collection was available, only the real-time display reading. The working distance was adjusted in a trial at the intended gas flow to make sure a stable plasma is produced with the H_2 gas. This trial led to a working distance of around 8-9 mm. The plasma generator sets the required voltage to ignite the plasma. The plasma current was then set to 300 mA, targeting a power of around 100 W. Depending on the gas flow ratio the voltage needed to maintain the plasma varies somewhat, the resulting power remained in a range between 92-105 W. Pressure in the chamber was set to 8 Torr but with actual pressure around 7.7 ± 0.1 Torr. The total gas flow was set at 1440 sccm for all experiments. In the first phase of experiments a deposition time of 15 min was used for all samples while the temperature was set to 550 or 590 °C and C_2H_2:H_2 ratio was varied in a range between 1:3.5 and 1:60. In the second experimental phase gas ratio was set to 1:40. The growth time was extended up to 60 minutes in increments of 15. The temperature dependency was investigated by comparing 30 minute growth at 470, 510, 550 and 590° C.

Before growth, 1x1 cm^2 PTL substrates were cut from a larger sheet and cleaned in an ultrasonic bath using acetone, isopropyl alcohol, methanol, and de-ionized water, for 10 minutes each time. The frequency was set to 35 kHz with constant sonication and no additional heating. After cleaning they were dried on a hot plate (130 °C) for around 1-2 minutes.

After cleaning, catalyst films were deposited using an e-beam evaporator (Lesker PVD 225). One such sample after Fe deposition is shown in Figure 4. Due to availability of source materials, two different PVD tools of the same model were used for depositing Ni and Fe respectively. During deposition a target is heated by an electron beam to a temperature where atoms evaporate towards the sample holder and are deposited on the surface, forming a thin film. A quartz crystal microbalance is used to establish a steady deposition rate of 1 Å/s. When the deposition rate is steady a shutter opens and deposition onto the samples proceeds while monitoring the thickness of the deposited film. For both Ni and Fe film deposition, 22 samples were placed on a 6-inch sample holder and coated at the same time.

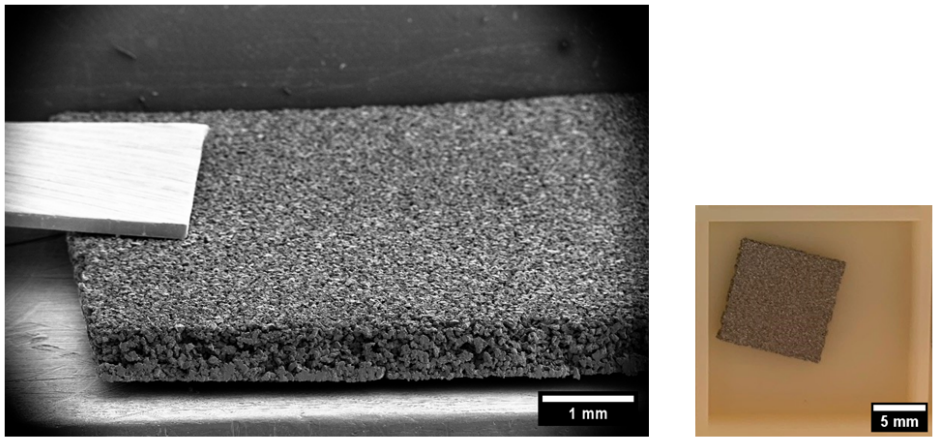

Figure 4: a) Low-magnification image from SEM showing the PTL substrate. b) Camera image of the PTL substrate after Fe deposition, as stored in sample container.

Samples were placed in the reaction chamber and annealed at a base pressure of <10 mTorr during ramp up to the growth temperature. On average the heating took around 15-20 min and then the chamber was kept at temperature for around 1 minute until the gas flow was opened. The time depended on the growth temperature but also the starting temperature that was around 20 °C for the first experiment of the day or around 150 °C for the subsequent experiments. After 1-1.5 minutes the pressure in the chamber had stabilized and the plasma was ignited, at which point the growth timer was started. Upon letting the gas flow into the reaction chamber, at process temperature of 550 °C, the heater temperature dropped by around 18 °C, compared to around 2 °C for a standard NH_3-process at Smoltek. This is attributed to the higher thermal conductivity of H_2 as compared to NH_3 [32]. As the growth time ends, the gas flow, plasma power supply, and heater were shut off and the reactor was left to cool down at a low pressure. After

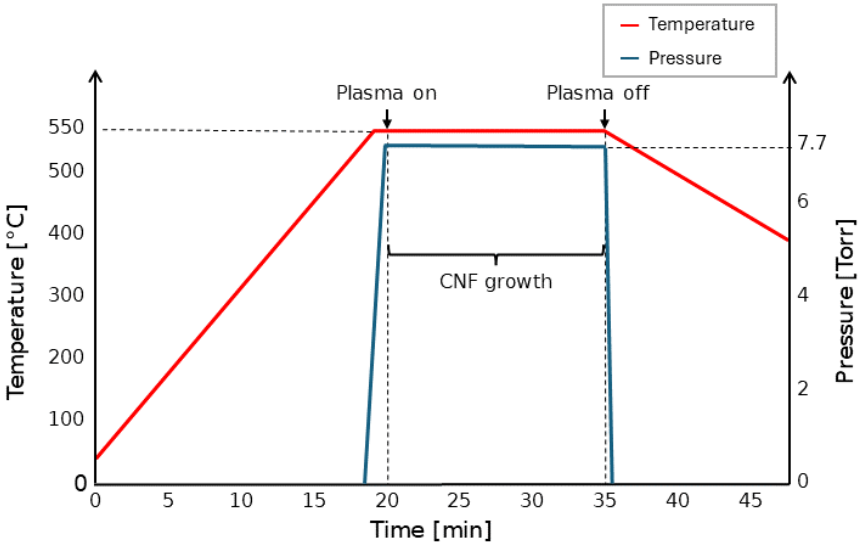

Figure 5: Schematic plot of the temperature and pressure in the PECVD reactor during an experiment. No data to plot the real variation over time is available.

around 2 hours the temperature had dropped to around 150-200 °C and the chamber could be vented for samples to be taken out. Venting further decreased the temperature so that handling was safe.

Characterization was performed using a Zeiss Supra 60 VP SEM and a Jeol JEM 3000F TEM/scanning TEM (STEM) equipped with an EDX detector. TEM samples were prepared by carefully scraping off deposited carbonaceous material from the surface of the samples using a scalpel knife, the scraped-off material was transferred to a TEM grid soaked in ethanol to aid adhesion of the carbonaceous material to the TEM grid. Using HRTEM images the crystal structure of the catalyst was analyzed by doing a fast Fourier transform (FFT) and measuring the distance from the origin to the observed lattice reflections in the reciprocal space as well as the angle between these reflections. The results were compared to standard structures. Length, diameter and density of CNFs was later measured from SEM micrographs using the software ImageJ [33]. For the density measurement, an adaptive threshold script was used which scans the image and creates a binary image by comparing local intensity variations [34]. From the binary image the number of particles could be counted by the built-in "Analyze Particles" function in ImageJ. A more detailed explanation of the steps is included in Appendix I.

5 Results

During the initial phase CNFs were successfully synthesized in a uniform manner on the PTL using Fe as catalyst. A summary of the initial experiments is presented in Table 1. Worth noting is that no successful synthesis occurred using Ni as catalyst and for the samples where some growth happened it was very non-uniform and with poor or no vertical alignment. The results from the Ni-catalyzed growth are briefly discussed later in section 5.4. The results discussed in this section should be considered in the light of remaining necessary optimization and some questions about reproducibility presented in section 5.3.

*Table 1: Summary of experiments done in the first phase studying effect of catalyst, temperature and ratio on the growth. Growth time was 15 min for all samples. There is a large variation in terms of density and morphology for CNFs. * Failed catalyst deposition. ** No SEM analysis done.*

Growth Temp [°C]	**Gas Ratio**	**Average plasma power [W]**	**Fe-catalyzed CNF growth**	**Ni-catalyzed CNF growth**
590	1:3.5	127	No	No
590	1:17	105	Very few	Sparse
550	1:23	98	Sparse	*
550	1:35	102	Semi-dense	Sparse
590	1:35	99	Sparse	Few patches of growth
550	1:40	95	Dense	Very few
550	1:45	93	Dense	Sparse
590	1:45	92	Very few	Few
550	1:50	98	Dense	Sparse
550	1:60	93	Very few	**

In all initial experiments, plasma was successfully created and some carbonaceous deposition occurred. The average plasma power was overall rather similar with a vague trend of dropping with higher ratio. The plasma coverage changes somewhat with the ratio, a detailed discussion and study of the plasma behavior is outside the scope of this thesis but two examples of its appearance during growth are shown in Figure 6 with annotations to explain different parts of the reactor. Additional images showing some more in-depth observations of the variation with gas ratio and temperature are included in appendix II.

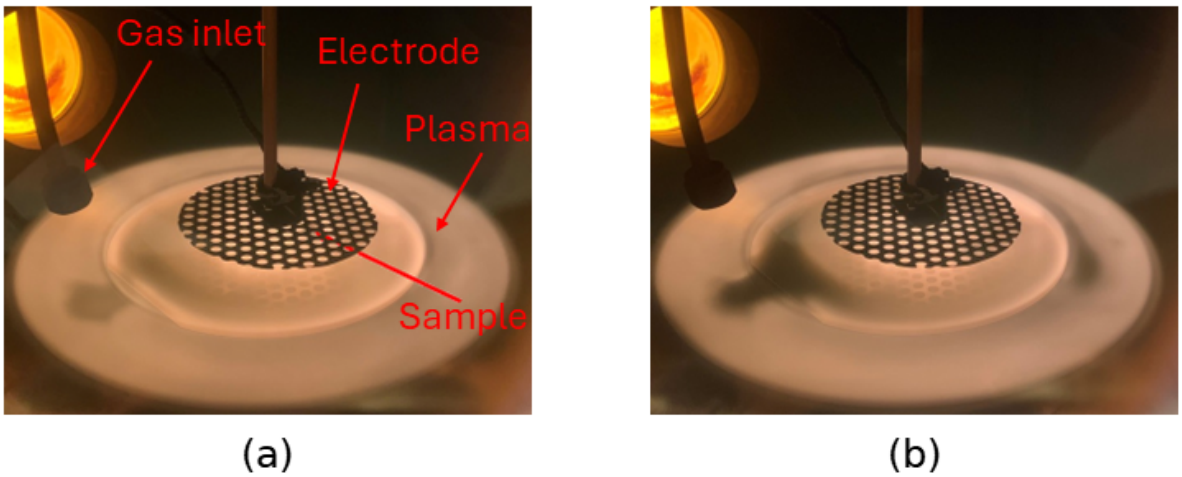

Figure 6: Images showing the plasma during CNF growth. The plasma covers the heater. Both images taken 3 minutes in to 15 minute growth time. (a) Experiment with C_2H_2:H_2 ratio of 1:40, 550 °C. (b) Experiment with C_2H_2:H_2 ratio of 1:45, 550 °C.

5.1 Fe-catalyzed growth

Micrographs of the Fe-coated samples are shown in Figure 7 and Figure 8, grouped by growth temperature. The growth at 590 °C showed considerably poorer results compared to 550 °C. During the lower temperature experiments, the growth appears rather robust to the ratio and similar results were achieved between ratios 1:35 and 1:50. It is worthwhile to note that these are rather small changes. This is perhaps better illustrated using percentages: the ratio of 1:35 is equivalent to 2.78 % C_2H_2 and 1:50 is equivalent to 1.97 % C_2H_2 in the gas mixture.

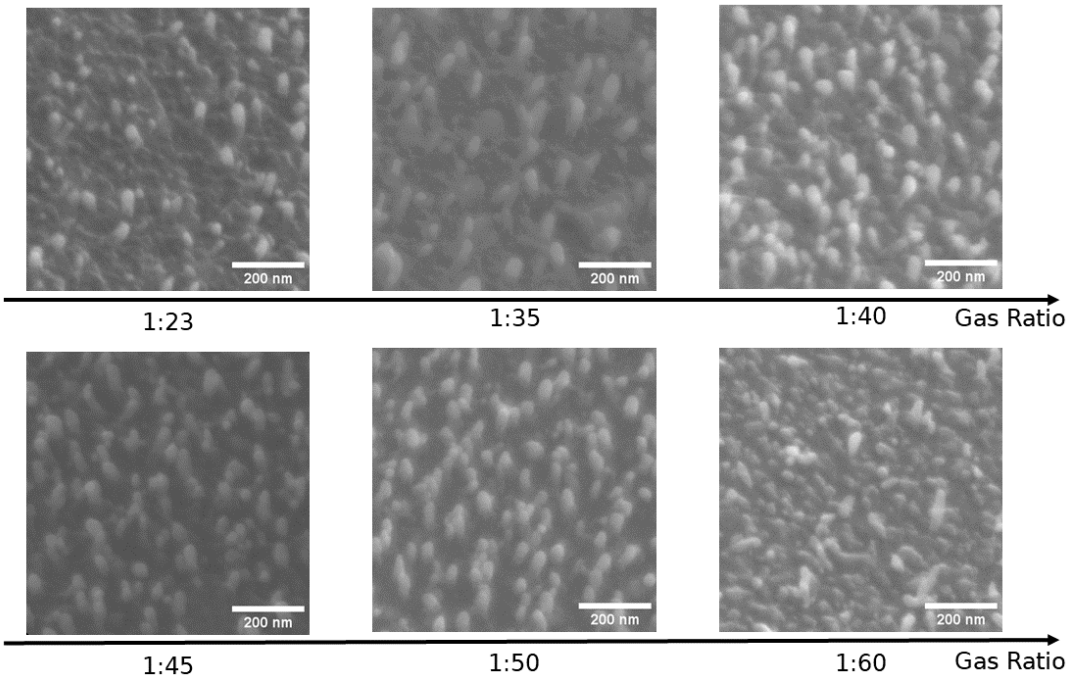

Figure 7: Micrographs showing samples with grown CNFs. Growth at 550 °C, 15 min, and different gas ratios. All images were taken at 30° angle and 70kx magnification.

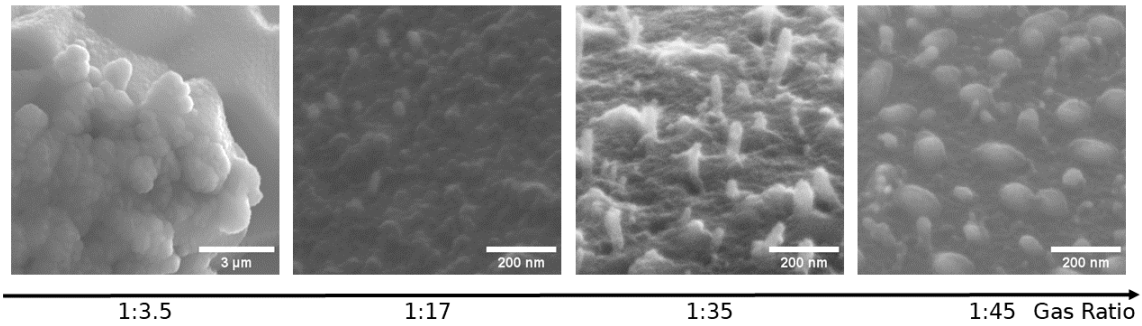

Figure 8: Micrographs showing growth at 590 °C, 15 min and different gas ratios. Far left image taken from a top view at 5kx magnification. The other images were taken at 30° angle and 70kx magnification.

In Figure 9, the length and density of fibers depending on the precursor gas ratio is shown. A range around the gas ratio 1:40 produced fairly similar results. The optimal ratio appeared to be 1:40 based on a combination of CNF length and density, with an important caveat that during this growth the temperature ramp up time was extended by around 25 minutes compared to the normal 15-20 minutes due to the heater malfunctioning. The diameter did not exhibit any trend with respect to the gas ratio with average diameter staying in a range between 28.3 and 34 nm. The potential influence of this is discussed in section 6.

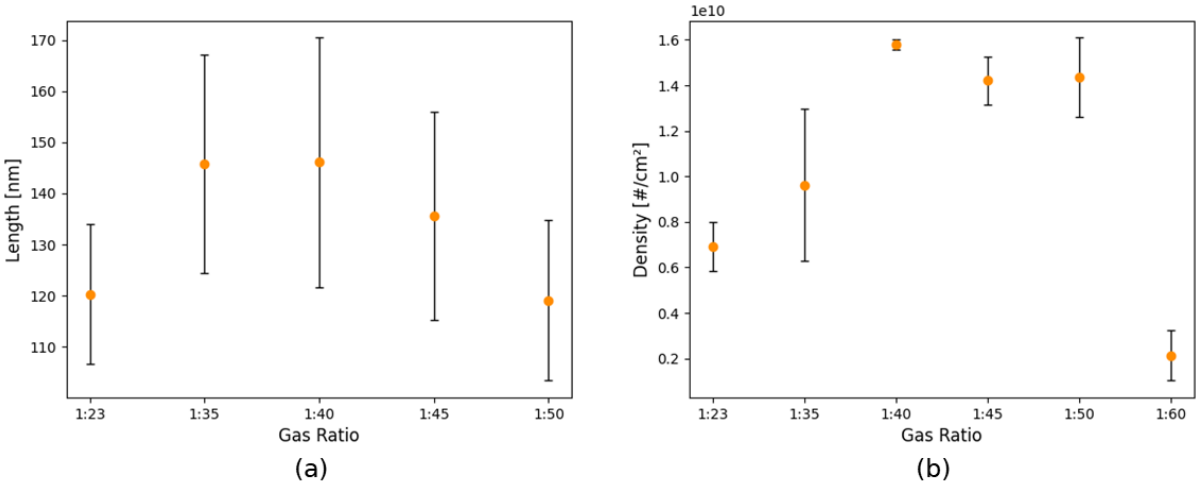

Figure 9: a) CNF length in nm for different target gas ratios, C2H2:H2 in the precursor gas mixture after 15 minutes growth. Measured at 2-3 positions for each sample. Error bars show standard deviation. b) CNF density for different target gas ratios, C2H2:H2 in the precursor gas mixture after 15 minutes growth. Measured at 2-3 positions for each sample. Error bars show standard deviation.

At the ratio of 1:40 the CNF growth rate, assuming a steady rate, is around 9.7 nm/min. To investigate the growth mode TEM analysis was also performed on this sample. Only three fibers were clearly observed. One example is shown in Figure 10. The length of this fiber is similar to the longest ones measured from SEM images, indicating that the whole fiber has detached from the substrate, although that is difficult to verify. An EDX spectra was taken of a region of this fiber, and it was confirmed that the dark contrast observed is Fe. The elongated Fe catalyst is

around 210 nm and the whole fiber 240 nm long. Furthermore, HRTEM shows graphitic layers on the side with the distance between 10 layers measured, giving an interlayer spacing of 3.6 Å.

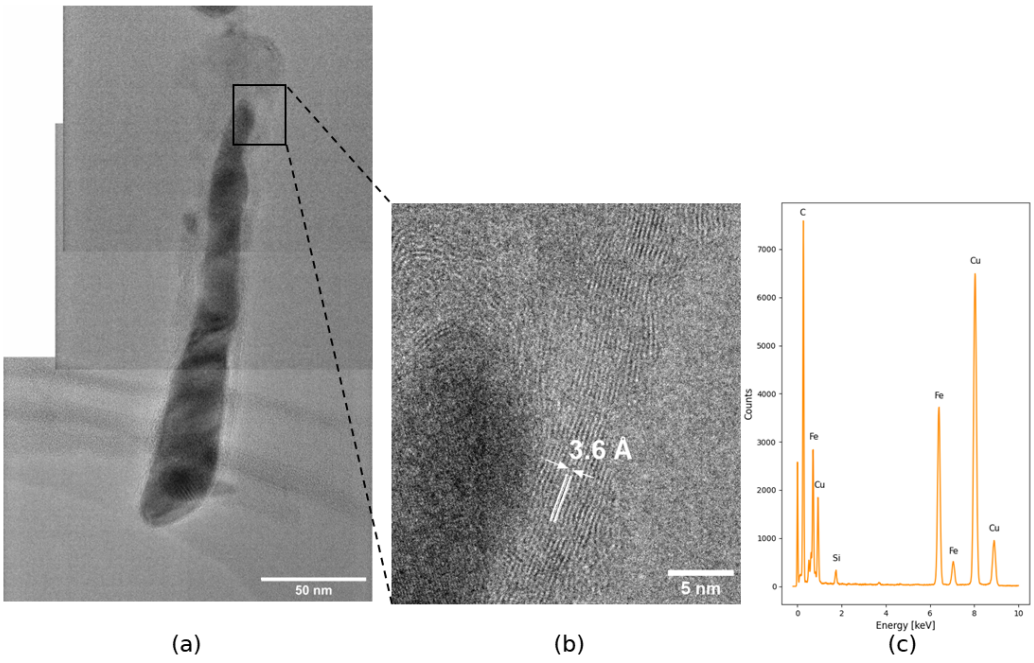

Figure 10: a) TEM composite showing CNF grown at gas ratio of 1:40 at 550 C for 15 minutes. b) HRTEM showing graphitic sheets of carbon on the side of the same CNF. The distance between 10 layers was measured yielding an interlayer spacing of 3.6 Å. c) EDX spectra from the same fiber, showing the presence of Fe and C. Cu-signal is from the TEM grid and there was some Si contamination on the TEM grid which could explain the weak Si-signal observed.

To further investigate the phase of the catalyst particle high resolution images were captured in order to analyze interplanar distances and compare with values for low-index planes in α-Fe, ɣ-Fe and Fe_3C respectively. The HRTEM image and FFT is shown in Figure 11**Error! Reference source not found.**, from the measured distances metallic Fe could be excluded due to the 3.36 Å distance which is not found in the structures of either α-Fe or ɣ-Fe. Oxides were deemed unlikely due to the lack of oxygen signal in the EDX spectra, shown in Figure 10, and it was difficult to match planes for common oxides as well. The distances found matched most closely with Fe_3C and the (210), (002) and (212) planes with mismatch of -1.67%, -0.41% and 4.75 % respectively. The angles between the planes are also mismatched compared to the conventional standard structure [35]. In the FFT image the angle between the proposed (002) and (212) plane is 63.7° and between (002) and (210) 97.5°. From the conventional standard structure, the angle between the same planes is 58.6° and 90° respectively.

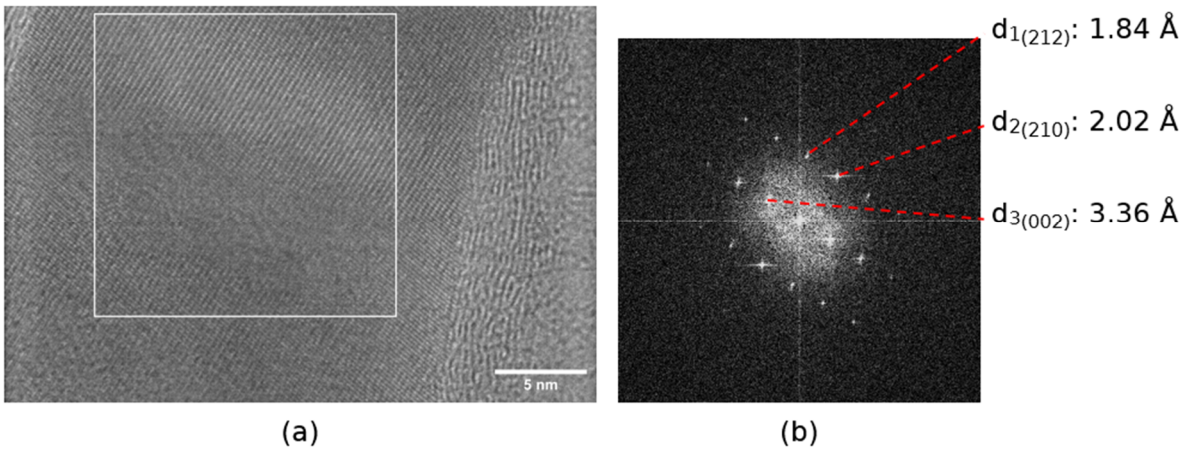

Figure 11: a) HRTEM image of the CNF shown in figure 10, ROI for FFT highlighted in white. b) FFT showing pattern and measured distances highlighted together with closest matching planes in a Fe_3C crystal.

5.2 Film growth

Comparing the initial and later phase of experiments, two distinct regimes of growth were observed. The difference is seen in Figure 12 by comparing two samples grown using the same experimental parameter settings. In Figure 12b one can observe CNFs growing within craters of a surrounding smooth film. This type of film growth surrounding the CNFs is clearly observed for 7 out of the 9 last samples grown. For the first 10 samples, this film is not visible. This change in growth behavior is further illustrated by a lower CNF density, as shown in Figure 13. Compared with early experiments around the 1:40 ratio the density is lower by around a factor of three in the film growth regime.

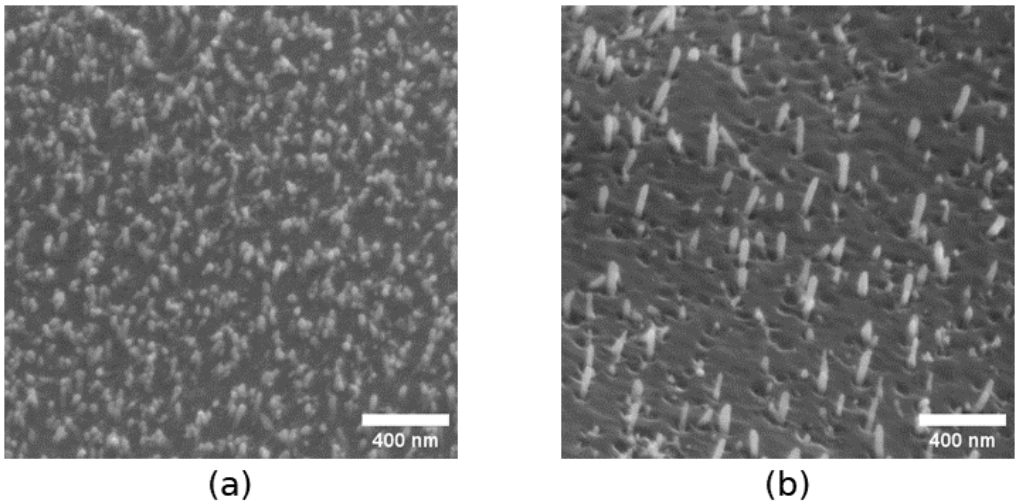

Figure 12: SEM Micrographs showing two samples grown at the same conditions: 15 minutes, 550 °C, 1:40 ratio. (a) Sample from initial experiments at gas ratio 1:40, 550 °C and 15 minutes of growth. Image taken at 30° angle, 30kx magnification. (b) Re-run with the same experimental settings during second phase of experiments. Image taken at 55° angle, 30kx magnification.

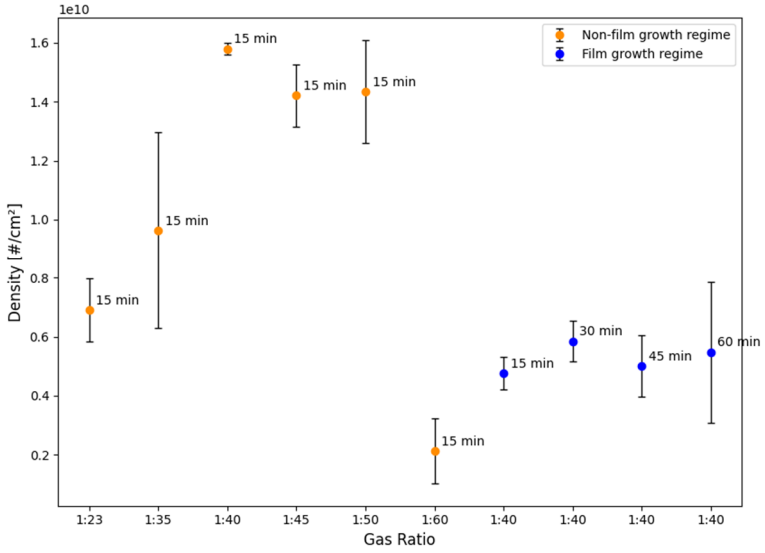

Figure 13: CNF density for different target gas ratios, C_2H_2:H_2 for the initial experiments, pre film growth observation, in orange. Later experiments, post film growth, in blue. Annotated with growth time. Measured at 2-3 positions for each sample. Error bars show standard deviation.

The film growth shown above dominates over CNF growth at lower temperatures, hindering the study of temperature dependency for the CNF growth. Figure 14 shows a series of experiments at a temperature ranging from 470 °C to 590 °C. At 510 °C the sample is largely covered with a smooth film covering the fibers which appeared translucent from a top view (See appendix 3). At 470 °C the film is thicker and no longer translucent from the top view. Figure 14a shows a hole in the smooth film and some fiber-like growth within the hole, 14b shows an edge of the smooth film and an area where some fiber-like growth was observed. The measured film thickness is 83 ± 7 nm and 216 ± 17 nm at 510 and 470 °C respectively.

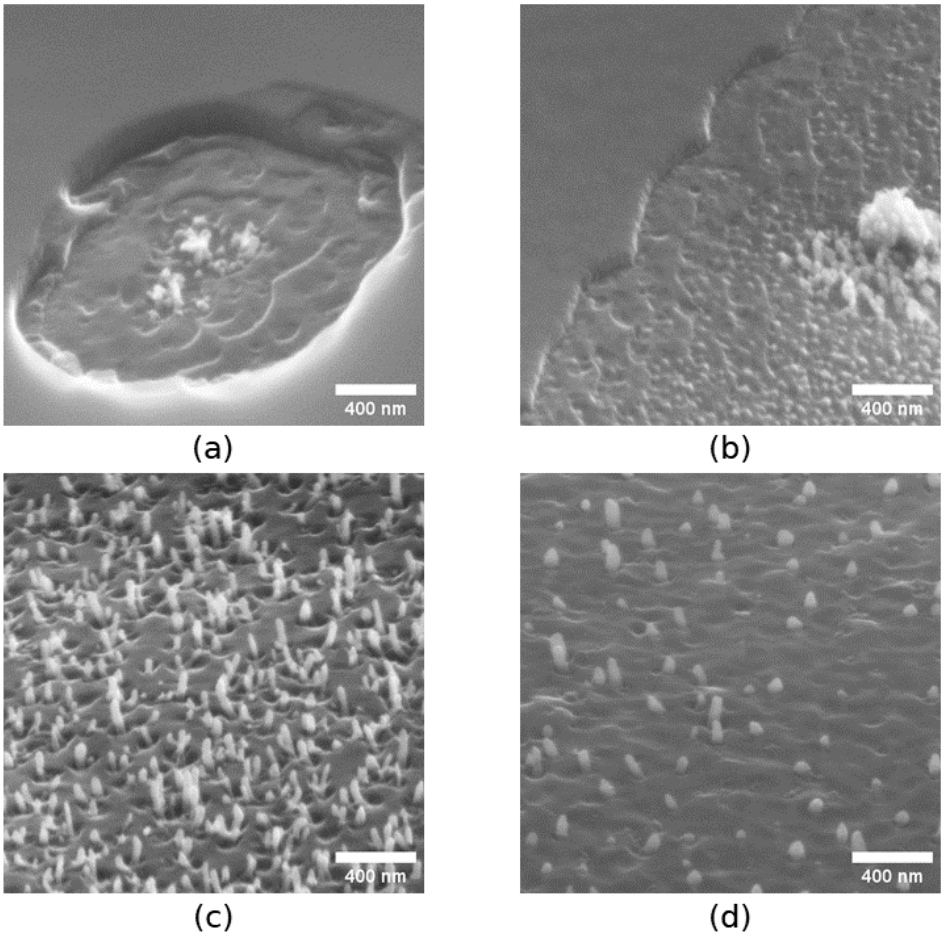

Figure 14: Film growth at different temperatures. All samples grown at gas ratio 1:40 for 30 min. (a) 470° C. Image taken at 55° angle, 30kx magnification. (b) 510° C. Image taken at 55° angle, 30kx magnification. (c) 550° C. Image taken at 55° angle, 30kx magnification. (d) 590° C. Image taken at 55° angle, 30kx magnification.

One sample grown at 550 °C for 45 minutes with gas ratio 1:40, was observed in the TEM. For this sample, which also exhibited film growth when observed in SEM, isolated fibers were not found but instead whole Ti-grains with the CNF growth on top. Figure 15 shows such a grain and the results of STEM-EDX mapping. The EDX analysis confirms that the grain observed is Ti and the presence of both Fe and C. It can also be observed that some of the Fe-catalyst is still left on the substrate after growth, whilst some is concentrated towards the top of the deposited carbon.

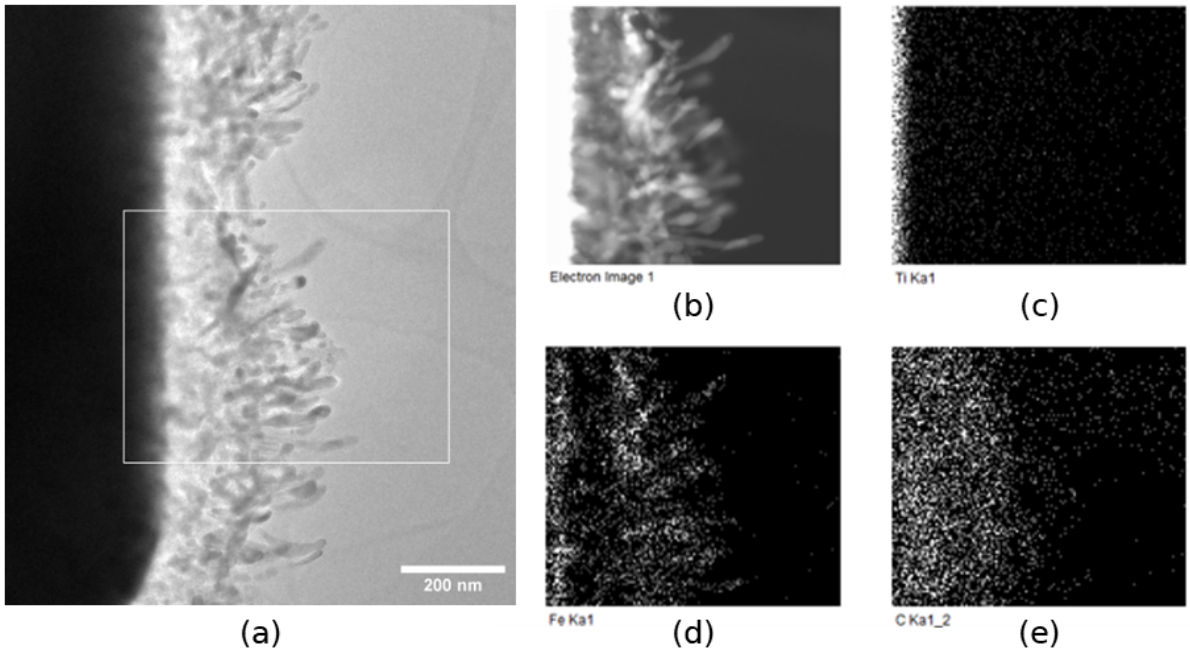

Figure 15: a) TEM image showing the Ti grain with carbon deposition on top. The highlighted area was selected for STEM-EDX mapping. Image taken at 12 kx. b) High-angle annular dark field image of the area highlighted in a) taken in STEM mode. c) STEM-EDX mapping of Ti. d) STEM-EDX mapping of Fe. e) STEM-EDX mapping of C.

5.3 Reproducibility

In the second experimental phase, as the growth time and temperature range were extended results were difficult to analyze due to issues with uniformity, non-vertically aligned growth and the above-mentioned film growth. It was not possible to reproduce the results seen in the initial phase.

The non-uniformity is possibly linked to a bending of samples during the growth which was observed for 9 out of 11 samples grown at higher temperature (590 °C) or for longer growth times (30 minutes or more). This bending also correlated with a ring pattern of growth with different morphology and density on different parts of the sample. An example of this is shown in Figure 16 from a sample where SEM images were taken to observe the difference between the darker and the brighter regions on the sample. This sample had a very clear ring pattern, on other samples where this was observed it was less pronounced and therefore also more difficult to capture with the camera.

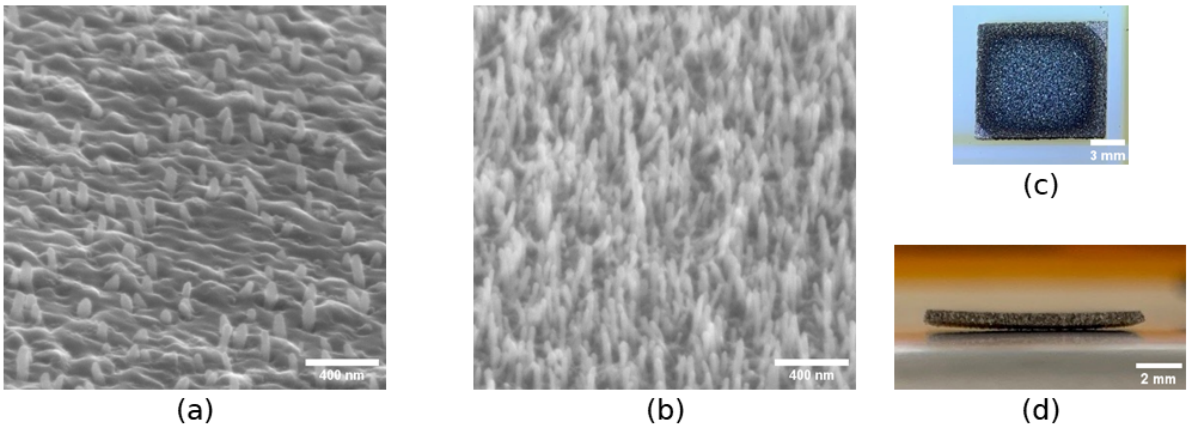

Figure 16: Non-uniform CNF growth and bending of sample for growth at ratio 1:40, 590° C, 30 min. (a) Micrograph of CNF growth in center of PTL substrate. Image taken at 50° angle, 30kx magnification. (b) Micrograph of CNF growth in dark ring region of PTL substrate. Image taken at 50° angle, 30kx magnification. (c) Camera image of sample taken showing a dark ring region close to the edge and brighter areas in the middle and at the edge. (d) Camera image showing a side view of the sample where bending can be observed.

5.4 Ni-catalyzed CNF growth experiments

For all tested experimental conditions, the Ni-coated samples only showed patchy or sparse non-vertically aligned growth, so eventually this route was abandoned. Figure 17 shows two examples from the trials. Figure 17a also appears to show a film growing on the substrate, possibly similar to the one observed for the Fe-coated samples.

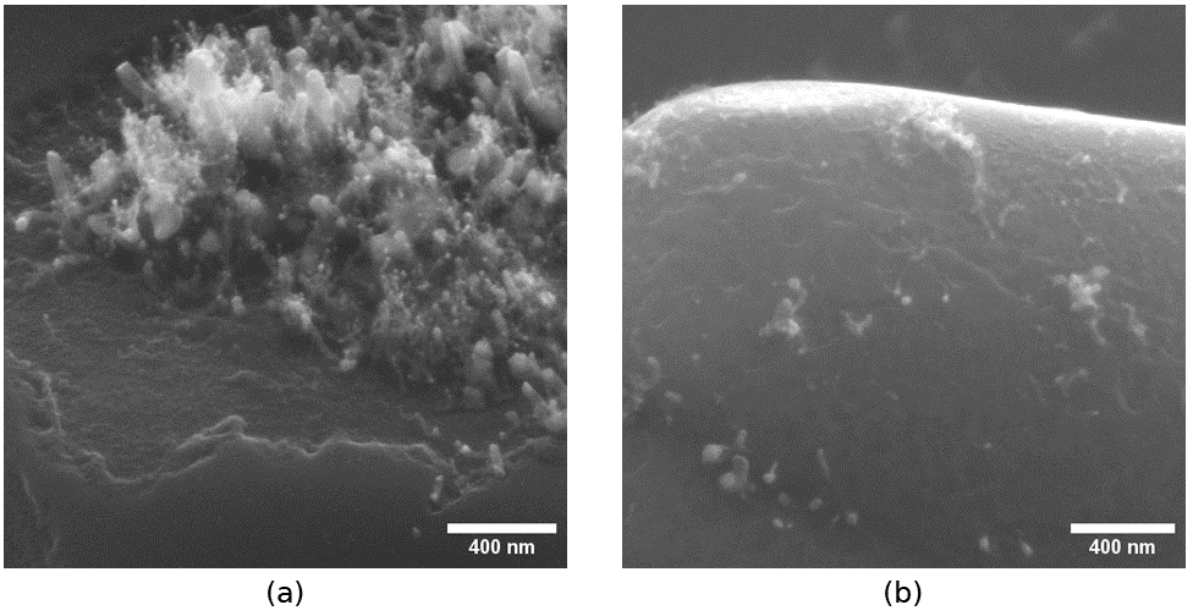

Figure 17: a) SEM micrograph showing a patch with CNF growth on a Ni-coated sample. Grown at 590 °C, gas ratio 1:35 for 15 minutes. Image taken at 45° angle, 30kx magnification. b) SEM micrograph showing sparse non-vertically aligned CNF growth on a Ni-coated sample. Grown at 550 °C, gas ratio 1:40 for 15 minutes. Image taken from a top view, 30kx magnification.

6 Discussion

Vertically aligned CNFs have been grown on a PTL substrate using Fe as a catalyst. The behavior of the growth with changing gas ratio can be linked to the purpose of the two gases in the process. With a lower relative amount of H_2, ratios 1:3.5 – 1:23, there is no CNF growth or only sparse growth and the same is true at the opposite end at the ratio of 1:60. At the low ratio this could be explained by insufficient etching of the surface of the catalyst particles, leading to an amorphous carbon coverage and inhibition of growth. At the high ratio instead, the explanation can be that the etching is too strong and/or that the supply of carbon is too low, thus inhibiting the growth of amorphous carbon but of the CNF as well. The proper condition for optimizing the growth is then found at a good balance of carbon supply and etching. This matches the argument in Chhowalla et al. mentioned in section 2.1, and this result appears to show, perhaps as expected, that the same trend emerges for an Fe-catalyzed C_2H_2/H_2 process as for the Ni-catalyzed C_2H_2/NH_3 process considered in their study [11].

Based on the density of CNFs it appears that the catalyst particle formation is rather consistent during the initial phase of experiments when the non-film growth regime was observed. The density of CNFs is very similar for ratios 1:40, 1:45 and 1:50 at 550° C and it is worth noting that for the sample with ratio 1:60 there are particles seen of similar density to the CNFs at lower ratios but only some of which have CNFs growing on top. This is likely catalyst particles formed from the dewetting process, but CNF growth is inhibited due to strong etching. However, further studies could be useful to fully confirm this.

Another observation that invites further study is the shape of the catalyst particles shown in Figure 10. In literature two growth modes for CNFs are typically found, base-type and tip-type. The observation from this sample is difficult to place in either of these categories as the catalyst particle is highly elongated and follows the whole fiber. The observed graphitic layers with interlayer spacing fall within the range you would expect for CNTs [36]. A fitting description is rather a core-shell Fe/CNT fiber. For the other sample with observations from TEM no isolated fibers were found, only Ti grains as shown in Figure 15 - for this sample elongated Fe cores could be observed but only parts of fibers could be seen. Even if more observations would be needed to say whether this core-shell structure is there for all fibers it leads to interesting questions about how this might influence the growth. This catalyst shape could indicate a strong adhesion to the Ti substrate and if the Fe catalyst elongates along the whole fiber during growth Fe supply could be a limiting factor for the growth rate. Another explanation could be that the low growth rate is caused by something else, for example plasma conditions as discussed below, and that the core-shell morphology only emerges for short fibers and once the Fe-particles is stretched out to its maximum the fiber would grow in tip- or base-type mode. Similar core-shell structures have been reported previously in literature and covered in a few review papers. One review cites 14 studies exploring metal-filled CNTs [37], most of these use other synthesis methods and continuously supply the metal via an organometallic precursor, e.g. ferrocene. However, one study uses microwave PECVD and as catalyst deposits Pd by electrodeposition to grow Pd/CNT core-shell fibers, they suggest that the Pd filling of the CNTs can be explained by a capillary

effect. The authors also go on to describe a method of etching away the carbon shell to form Pd nanowires [38].

For the second phase of experiments the results were inconsistent and difficult to analyze, partly due to the film growth regime that was observed. At lower temperature the film growth dominated. The growth rate of the film seems to be inversely related to the temperature. Similar film growth has been reported previously by Melechko et al [39], describing it as a graphitic film. Based on the theory presented in the background the carbon film growth rate could be related to the etching properties of the plasma and this film growth might also inhibit the growth of CNF by covering the catalyst particle. Another proposal is that the film growth is related to the catalyst particle formation. The low density of CNF growth for these samples might be indicative of a change in the particle formation, either due to the dewetting process changing or due to an unexpected, systematic error in the deposited film thickness. The STEM-EDX in Figure 15, showing some Fe remaining on the substrate, could indicate that the catalyst was not efficiently used in the process, however there is no data from the non-film growth regime to compare with, limiting the conclusions that can be drawn from this observation. In summary, to conclusively answer why one regime with film growth and one without was observed, further studies are needed.

Apart from the film growth, variation in the density and morphology of CNFs over the same samples made quantitative analysis difficulty. This is likely related to the bending of samples that was observed. This is an issue that has not been as pronounced for the NH_3 process at Smoltek and it was not encountered during the literature review. Possibly it is related to the difference in thermal conductivity between H_2 and NH_3 gas, discussed briefly in section 4. Since H_2 gas is a better thermal conductor, the cold gas can more efficiently cool the substrate, as indicated by the cooling of the heater described in section 4, and this could create a thermal gradient between the center and edge of the PTL substrate. Such a gradient might induce bending of the sample. Also, the radial growth pattern that was observed is consistent with the cause being a thermal gradient. Understanding what causes both the bending and the two growth regimes, and how to influence this, should be of high priority in order to ensure reproducibility in the process.

The most important remaining questions after the findings presented above are how much more stable the process can get, with regards to temperature; and whether the growth rate can be improved. As mentioned above, the elongated catalyst particle could be related to the low growth rate but other aspects of the process can also be considered. One previous study achieves a growth rate close to 84 nm/min for a H_2-based process using Ni as catalyst and a pulsed DC plasma [30]. Baro et al compare growth rate between pulsed DC and DC plasma and in their study they show that the growth rate can be increased by up to 4 times by switching from DC to pulsed DC. They achieve a growth rate of around 67 nm/min [40]. These studies suggest switching to a pulsed DC system might improve the growth rate. Another proposal is that the experiments have been conducted at the edge of the growth parameter window in terms of one or several of the parameters not studied. This could explain both the lower growth rate and the

sensitivity to temperature observed. One such parameter that might be of particular interest is the plasma power. As mentioned in the method the plasma current was set with the aim to get around 100 W in power after considering the stability of the plasma in the PECVD reactor. The resulting plasma is quite large (see Figure 6 or appendix II). The actual area cannot be directly measured during each experiment but a rough estimate, based on the heater diameter which is 22.5 cm, yields a plasma area of around 400 cm^2. This gives a plasma power density of around 0.25 W/cm^2. The power density is not often reported in literature, but this value can be compared with Morjan et al, that report growth of dense CNT forests using PECVD with a plasma density of 2-4 W/cm^2 [41].

A rough estimate of the surface area enhancement from the grown CNFs can be calculated from the average length and diameter of the CNFs and the density. If this is done by assuming cylindrical shapes of the CNFs, the surface area is increased by around a factor of 3 for the 15 minute growth at 1:40 ratio and 550° C. This is with an average length of only 146 nm. The added surface area is proportional to the length of the fibers so if the growth rate can be improved the surface area enhancement will improve as well. In the current ammonia-based process at Smoltek, fibers with length of around 3-4 µm can easily be achieved [42]. However, these fibers tend to entangle and form clusters, effectively reducing the surface area enhancement. If it is possible to increase the length of the CNFs produced in this project and avoid entanglement and cluster formation this could prove to be an advantage of the H_2 process.

7 Conclusions and outlook

The experimental work done for this thesis project has laid a good foundation for continued experiments and showed that growing Fe-catalyzed vertically aligned CNFs on porous titanium using H_2 is possible. Further studies are needed to ensure reproducibility and to improve the growth rate. Several important parameters are left out of this study due to time limitations, especially the catalyst film thickness and the plasma parameters are likely to have a large influence on the resulting growth.

Several key experiments can be identified to further the understanding of this process and to improve it. High resolution EDX and/or atomic force microscopy studies might shed some light on the catalyst particle formation. Studies of dewetting at different temperatures and times could provide ways to increase the control of the CNF density. The catalyst particle formation is one possible explanation for the film growth/non-film growth regime and if so, this might be possible to control by better understanding the dewetting process and the influence of the film thickness. Another thing to study is the bending of the samples, when it occurs and how to avoid it. These are important measures to achieve a stable growth process.

The appearance of the catalyst particle in TEM, as mentioned in section 6, would be interesting to revisit in light of attempts to increase the growth rate. If the observed morphology is consistent throughout the samples, this might be a limiting factor for the growth rate since Fe is not

continuously supplied during the reaction. This also ties into the catalyst film deposition and particle formation and whether the adhesion to the titanium can be affected, for example by pre-treating the substrate before catalyst film deposition or the catalyst before growth. One such pre-treatment of the catalyst is to ignite a plasma with only the H_2 gas and expose the samples to this before introducing the carbon precursor gas. Hash et al suggest that ion bombardment from a plasma can loosen catalyst particles and promote tip growth [13]. A few studies do some sort of plasma pre-treatment before growth [24], [43]. If such pre-treatment could loosen the Fe catalyst and change the growth to tip-mode, this could be a promising route to improve the growth rate.

Some new issues might arise with the use of hydrogen such as hydrogen embrittlement of the Ti substrate. This would also be interesting to study in the future.

Overall, there are some remaining challenges before the CNF growth with NH_3 can be replaced by H_2. However, there are some clear routes identified for tackling these challenges. Additionally, the core-shell Fe/CNT structures that were observed in TEM could be interesting for applications where the magnetic properties of the Fe core can be used and could merit further study in themselves. It is also worth noting that the large plasma that is easily produced in the H_2-based process might prove useful in attempts to scale up the sample size for larger scale electrolysis cell applications.

References

[1] H. Kojima, K. Nagasawa, N. Todoroki, Y. Ito, T. Matsui, and R. Nakajima, "Influence of renewable energy power fluctuations on water electrolysis for green hydrogen production," *Int. J. Hydrog. Energy*, vol. 48, no. 12, pp. 4572–4593, Feb. 2023, doi: 10.1016/j.ijhydene.2022.11.018.

[2] P. Shirvanian and F. van Berkel, "Novel components in Proton Exchange Membrane (PEM) Water Electrolyzers (PEMWE): Status, challenges and future needs. A mini review," *Electrochem. Commun.*, vol. 114, p. 106704, May 2020, doi: 10.1016/j.elecom.2020.106704.

[3] M. Clapp, C. M. Zalitis, and M. Ryan, "Perspectives on current and future iridium demand and iridium oxide catalysts for PEM water electrolysis," *Catal. Today*, vol. 420, p. 114140, Aug. 2023, doi: 10.1016/j.cattod.2023.114140.

[4] C. Minke, M. Suermann, B. Bensmann, and R. Hanke-Rauschenbach, "Is iridium demand a potential bottleneck in the realization of large-scale PEM water electrolysis?," *Int. J. Hydrog. Energy*, vol. 46, no. 46, pp. 23581–23590, Jul. 2021, doi: 10.1016/j.ijhydene.2021.04.174.

[5] B. A. Cruden, A. M. Cassell, D. B. Hash, and M. Meyyappan, "Residual gas analysis of a dc plasma for carbon nanofiber growth," *J. Appl. Phys.*, vol. 96, no. 9, pp. 5284–5292, Nov. 2004, doi: 10.1063/1.1779975.

[6] D. Yadav, F. Amini, and A. Ehrmann, "Recent advances in carbon nanofibers and their applications – A review," *Eur. Polym. J.*, vol. 138, p. 109963, Sep. 2020, doi: 10.1016/j.eurpolymj.2020.109963.

[7] J. C. Ruiz-Cornejo, D. Sebastián, and M. J. Lázaro, "Synthesis and applications of carbon nanofibers: a review," vol. 36, no. 4, pp. 493–511, 2020, doi: 10.1515/revce-2018-0021.

[8] T. V. Hughes and Chambers, C. R., "Manufacture of carbon filaments." U.S. patent 405,480, Jun. 18, 1889.

[9] S. Iijima, "Helical microtubules of graphitic carbon," *Nature*, vol. 354, no. 6348, pp. 56–58, Nov. 1991, doi: 10.1038/354056a0.

[10] M. Amin Saleem, "Carbon nanomaterial-based interconnects, integrated capacitors and supercapacitors." Doktorsavhandlingar vid Chalmers tekniska högskola.

[11] M. Chhowalla *et al.*, "Growth process conditions of vertically aligned carbon nanotubes using plasma enhanced chemical vapor deposition," *J. Appl. Phys.*, vol. 90, no. 10, pp. 5308–5317, Nov. 2001, doi: 10.1063/1.1410322.

[12] V. I. Merkulov, A. V. Melechko, M. A. Guillorn, D. H. Lowndes, and M. L. Simpson, "Alignment mechanism of carbon nanofibers produced by plasma-enhanced chemical-vapor deposition," *Appl. Phys. Lett.*, vol. 79, no. 18, pp. 2970–2972, Oct. 2001, doi: 10.1063/1.1415411.

[13] D. B. Hash and M. Meyyappan, "Model based comparison of thermal and plasma chemical vapor deposition of carbon nanotubes," *J. Appl. Phys.*, vol. 93, no. 1, pp. 750–752, Dec. 2002, doi: 10.1063/1.1525854.

[14] A.-Y. Lo, S.-B. Liu, and C.-T. Kuo, "Effect of Temperature Gradient Direction in the Catalyst Nanoparticle on CNTs Growth Mode," *Nanoscale Res. Lett.*, vol. 5, no. 9, p. 1393, Jun. 2010, doi: 10.1007/s11671-010-9648-4.

[15] A. V. Melechko, V. I. Merkulov, D. H. Lowndes, M. A. Guillorn, and M. L. Simpson, "Transition between `base' and `tip' carbon nanofiber growth modes," *Chem. Phys. Lett.*, vol. 356, no. 5, pp. 527–533, Apr. 2002, doi: 10.1016/S0009-2614(02)00406-2.

[16] R. T. K. Baker, M. A. Barber, P. S. Harris, F. S. Feates, and R. J. Waite, "Nucleation and growth of carbon deposits from the nickel catalyzed decomposition of acetylene," *J. Catal.*, vol. 26, no. 1, pp. 51–62, Jul. 1972, doi: 10.1016/0021-9517(72)90032-2.

[17] S. Hofmann, C. Ducati, J. Robertson, and B. Kleinsorge, "Low-temperature growth of carbon nanotubes by plasma-enhanced chemical vapor deposition," *Appl. Phys. Lett.*, vol. 83, no. 1, pp. 135–137, Jun. 2003, doi: 10.1063/1.1589187.

[18] H. Yoshida, S. Takeda, T. Uchiyama, H. Kohno, and Y. Homma, “Atomic-Scale In-situ Observation of Carbon Nanotube Growth from Solid State Iron Carbide Nanoparticles,” *Nano Lett.*, vol. 8, no. 7, pp. 2082–2086, Jul. 2008, doi: 10.1021/nl080452q.
[19] C. T. Wirth *et al.*, “The Phase of Iron Catalyst Nanoparticles during Carbon Nanotube Growth,” *Chem. Mater.*, vol. 24, no. 24, pp. 4633–4640, Dec. 2012, doi: 10.1021/cm301402g.
[20] Z. He, J.-L. Maurice, A. Gohier, C. S. Lee, D. Pribat, and C. S. Cojocaru, “Iron Catalysts for the Growth of Carbon Nanofibers: Fe, Fe3C or Both?,” *Chem. Mater.*, vol. 23, no. 24, pp. 5379–5387, Dec. 2011, doi: 10.1021/cm202315j.
[21] M. Cantoro *et al.*, “Effects of pre-treatment and plasma enhancement on chemical vapor deposition of carbon nanotubes from ultra-thin catalyst films,” *Diam. 2005*, vol. 15, no. 4, pp. 1029–1035, Apr. 2006, doi: 10.1016/j.diamond.2006.01.007.
[22] H. Sharma, A. K. Shukla, and V. D. Vankar, “Effect of titanium interlayer on the microstructure and electron emission characteristics of multiwalled carbon nanotubes,” *J. Appl. Phys.*, vol. 110, no. 3, p. 033726, Aug. 2011, doi: 10.1063/1.3622565.
[23] S. Vollebregt and R. Ishihara, “Carbon Nanotubes as Vertical Interconnects for 3D Integrated Circuits,” in *Carbon Nanotubes for Interconnects: Process, Design and Applications*, A. Todri-Sanial, J. Dijon, and A. Maffucci, Eds., Cham: Springer International Publishing, 2017, pp. 195–213. doi: 10.1007/978-3-319-29746-0_7.
[24] F. A. Ghavanini, M. Lopez-Damian, D. Rafieian, K. Svensson, P. Lundgren, and P. Enoksson, “Controlling the initial phase of PECVD growth of vertically aligned carbon nanofibers on TiN,” *Eurosensors XXIV Linz Austria 5-8 Sept. 2010*, vol. 172, no. 1, pp. 347–358, Dec. 2011, doi: 10.1016/j.sna.2011.04.036.
[25] X. Sun *et al.*, “The effect of catalysts and underlayer metals on the properties of PECVD-grown carbon nanostructures,” *Nanotechnology*, vol. 21, no. 4, p. 045201, Dec. 2009, doi: 10.1088/0957-4484/21/4/045201.
[26] H.-S. Yoo, S.-J. Lee, S.-K. Joo, and W.-Y. Sung, “Density control of carbon nanofibers on titanium buffer layer using electroplated Ni catalyst,” *J. Vac. Sci. Technol. B Microelectron. Nanometer Struct. Process. Meas. Phenom.*, vol. 26, no. 2, pp. 880–884, Apr. 2008, doi: 10.1116/1.2839888.
[27] S. J. Randolph *et al.*, “Controlling thin film structure for the dewetting of catalyst nanoparticle arrays for subsequent carbon nanofiber growth,” *Nanotechnology*, vol. 18, no. 46, p. 465304, Oct. 2007, doi: 10.1088/0957-4484/18/46/465304.
[28] L. N. Sacco, H. J. van Ginkel, and S. Vollebregt, “Synthesis of Carbon nanofibers (CNFs) by PECVD using Ni catalyst printed by spark ablation,” in *2022 IEEE 22nd International Conference on Nanotechnology (NANO)*, Jul. 2022, pp. 128–131. doi: 10.1109/NANO54668.2022.9928632.
[29] Y. S. Woo, D. Y. Jeon, I. T. Han, N. S. Lee, J. E. Jung, and J. M. Kim, “In situ diagnosis of chemical species for the growth of carbon nanotubes in microwave plasma-enhanced chemical vapor deposition,” *Diam. Relat. Mater.*, vol. 11, no. 1, pp. 59–66, Jan. 2002, doi: 10.1016/S0925-9635(01)00519-2.
[30] M. Shooshtari, L. N. Sacco, J. Van Ginkel, S. Vollebregt, and A. Salehi, “Enhancement of Room Temperature Ethanol Sensing by Optimizing the Density of Vertically Aligned Carbon Nanofibers Decorated with Gold Nanoparticles,” *Materials*, vol. 15, no. 4, 2022, doi: 10.3390/ma15041383.
[31] M. K. Tabatabaei, H. Ghafouri fard, J. Koohsorkhi, S. Khatami, and S. Mohajerzadeh, “Remote and direct plasma regions for low-temperature growth of carbon nanotubes on glass substrates for display applications,” *J. Phys. Appl. Phys.*, vol. 44, no. 11, p. 115401, Mar. 2011, doi: 10.1088/0022-3727/44/11/115401.
[32] Marcia Huber and Allan Harvey, *Thermal Conductivity of Gases*. CRC-Press, Boca Raton, FL, 2011. [Online]. Available: https://tsapps.nist.gov/publication/get_pdf.cfm?pub_id=907540
[33] C. A. Schneider, W. S. Rasband, and K. W. Eliceiri, “NIH Image to ImageJ: 25 years of image analysis,” *Nat. Methods*, vol. 9, no. 7, pp. 671–675, Jul. 2012, doi: 10.1038/nmeth.2089.
[34] Q. Tseng, “AdaptiveThreshold - ImageJ plugin.” [Online]. Available: https://sites.google.com/site/qingzongtseng/adaptivethreshold#h.jwj99g9czrew

[35] A. Jain *et al.*, “Commentary: The Materials Project: A materials genome approach to accelerating materials innovation,” *APL Mater.*, vol. 1, no. 1, p. 011002, Jul. 2013, doi: 10.1063/1.4812323.
[36] O. V. Kharissova and B. I. Kharisov, “Variations of interlayer spacing in carbon nanotubes,” *RSC Adv.*, vol. 4, no. 58, pp. 30807–30815, 2014, doi: 10.1039/C4RA04201H.
[37] U. K. Gautam *et al.*, “Recent developments in inorganically filled carbon nanotubes: successes and challenges,” *Sci. Technol. Adv. Mater.*, vol. 11, no. 5, p. 054501, Oct. 2010, doi: 10.1088/1468-6996/11/5/054501.
[38] L. H. Chan, K. H. Hong, S. H. Lai, X. W. Liu, and H. C. Shih, “The formation and characterization of palladium nanowires in growing carbon nanotubes using microwave plasma-enhanced chemical vapor deposition,” *Thin Solid Films*, vol. 423, no. 1, pp. 27–32, Jan. 2003, doi: 10.1016/S0040-6090(02)00966-5.
[39] A. V. Melechko *et al.*, “Vertically aligned carbon nanofibers and related structures: Controlled synthesis and directed assembly,” *J. Appl. Phys.*, vol. 97, no. 4, p. 041301, Feb. 2005, doi: 10.1063/1.1857591.
[40] M. Baro, D. Gogoi, A. R. Pal, N. C. Adhikary, H. Bailung, and J. Chutia, “Pulsed PECVD for Low-temperature Growth of Vertically Aligned Carbon Nanotubes,” *Chem. Vap. Depos.*, vol. 20, no. 4-5–6, pp. 161–169, Jun. 2014, doi: 10.1002/cvde.201307093.
[41] R. E. Morjan, V. Maltsev, O. Nerushev, Y. Yao, L. K. L. Falk, and E. E. B. Campbell, “High growth rates and wall decoration of carbon nanotubes grown by plasma-enhanced chemical vapour deposition,” *Chem. Phys. Lett.*, vol. 383, no. 3, pp. 385–390, Jan. 2004, doi: 10.1016/j.cplett.2003.11.063.
[42] A. M. Saleem *et al.*, “Low temperature and cost-effective growth of vertically aligned carbon nanofibers using spin-coated polymer-stabilized palladium nanocatalysts,” *Sci. Technol. Adv. Mater.*, vol. 16, no. 1, p. 015007, Feb. 2015, doi: 10.1088/1468-6996/16/1/015007.
[43] S. Vollebregt, J. Derakhshandeh, R. Ishihara, M. Y. Wu, and C. I. M. Beenakker, “Growth of High-Density Self-Aligned Carbon Nanotubes and Nanofibers Using Palladium Catalyst,” *J. Electron. Mater.*, vol. 39, no. 4, pp. 371–375, Apr. 2010, doi: 10.1007/s11664-010-1094-7.

Appendix I

For all density analysis the same magnification, 30kx, and top view angle was used for all samples. The analysis is done in a few steps in ImageJ:

I. Convert image to 8-bit
II. Crop to area of interest
III. Process image using AdaptiveThreshhold algorithm to create a binary image.
    a. Double check that the binary image corresponds well to the particles in the original image.
IV. Use ImageJ algorithm "Analyze Particles" to count the particles.
    a. For the algorithm a minimum size of 10 pixels^2 was used. And for samples exhibiting film growth a circularity of 0.20-1.00 was selected to avoid counting film edges as particles.

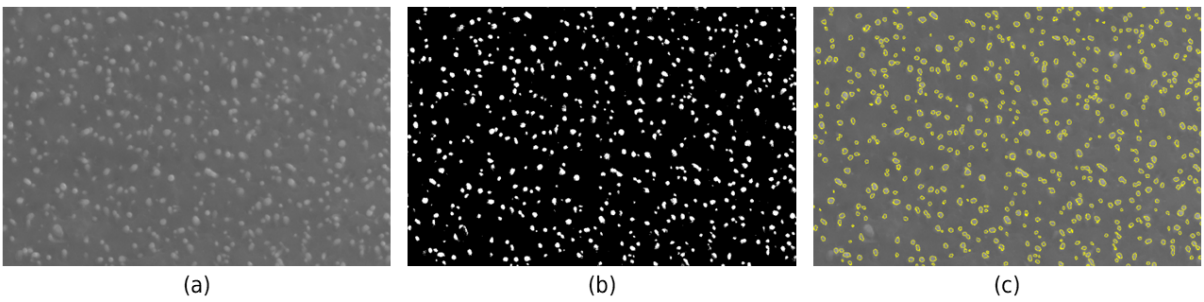

Figure 18: Image series showing how the density analysis is performed. (a) Original image, cropped. (b) Binary image after application of adaptive threshold algorithm. (c) Original image with particle overlay after application of "Analyze Particles"-algorithm.

Appendix II

The figures below show some examples of how the plasma varied in the chamber during experiments.

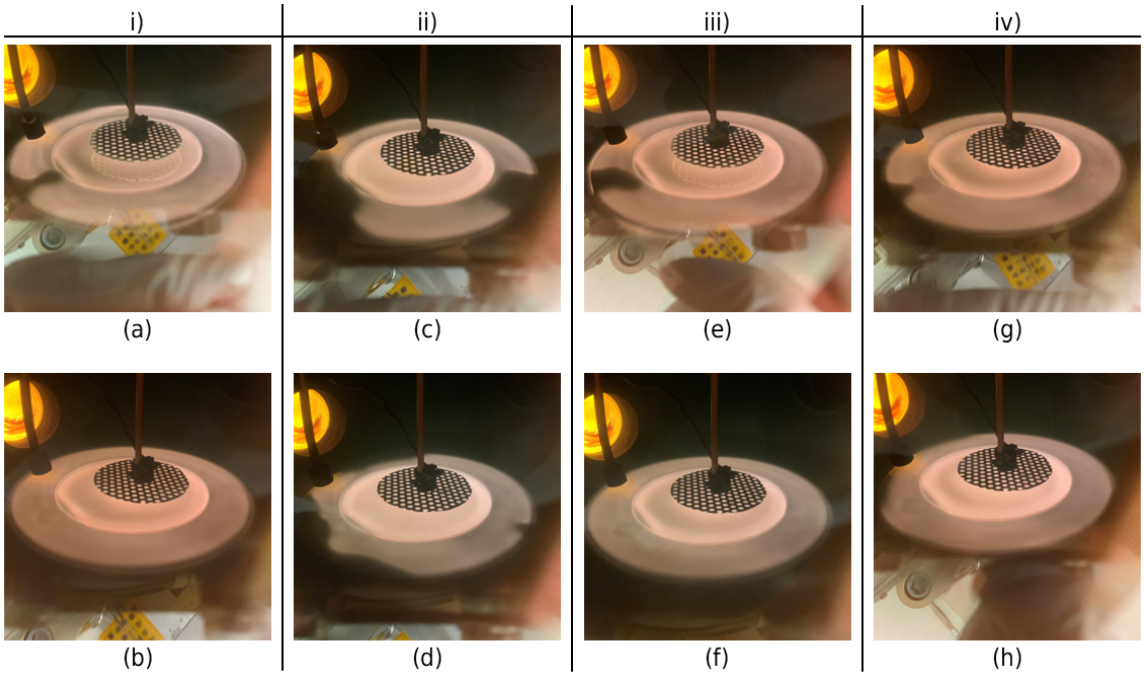

Figure 19: Plasma consistency. Photographic images of the plasma during growth. Experiments i-iv all done at 550° C, ratio 1:40 with total growth time: i) 15 min, ii) 30 min, iii) 45 min, iv) 60 min. Top images show the initial plasma and bottom images a few minutes into the growth. (a) After less than 1 minute. (b) After 6 minutes. (c) After less than 1 minute. (d) After 5 minutes. (e) After less than 1 minute. (f) After 7 minutes. (g) After less than 1 minute. (h) After 10 minutes.

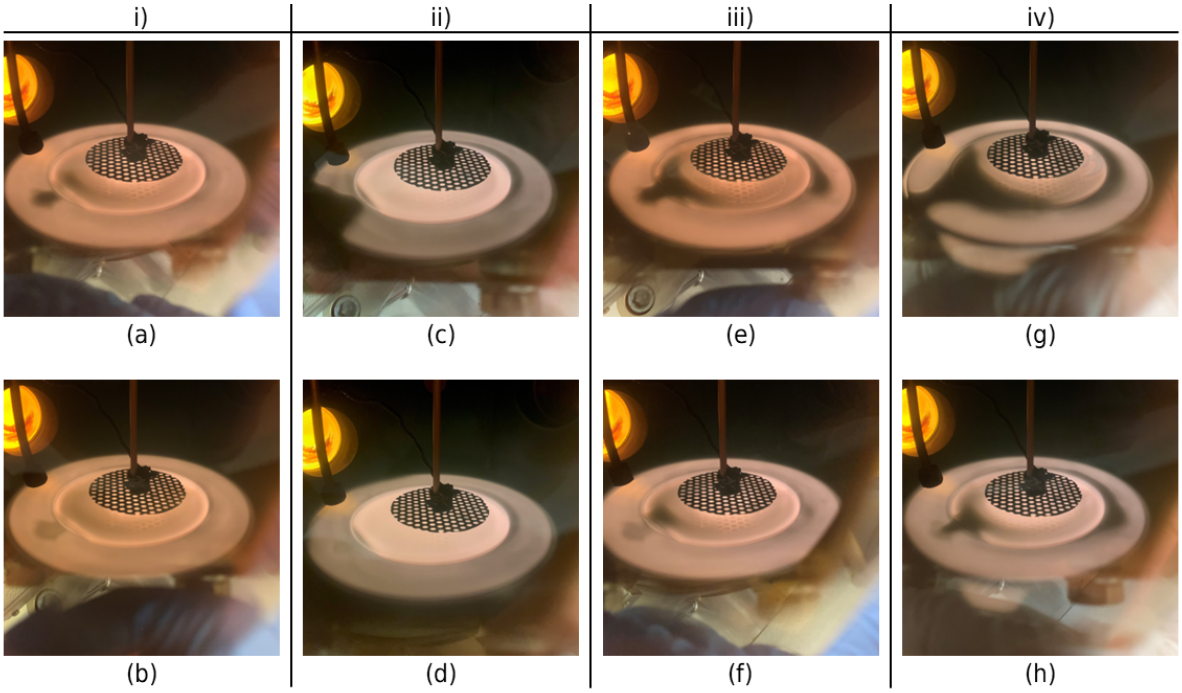

Figure 20: Influence of temperature on the plasma. Photographic images of the plasma during growth. Experiments i-iv done at different conditions: i) 550° C, ratio 1:40, ii) 590° C, ratio 1:40, iii) 550° C, ratio 1:45, iv) 590° C, ratio 1:45. Top images show the initial plasma and bottom images a few minutes into the growth. (a) After less than 1 minute. (b) After 6 minutes. (c) After less than 1 minute. (d) After 5 minutes. (e) After less than 1 minute. (f) After 7 minutes. (g) After less than 1 minute. (h) After 10 minutes.

Appendix III

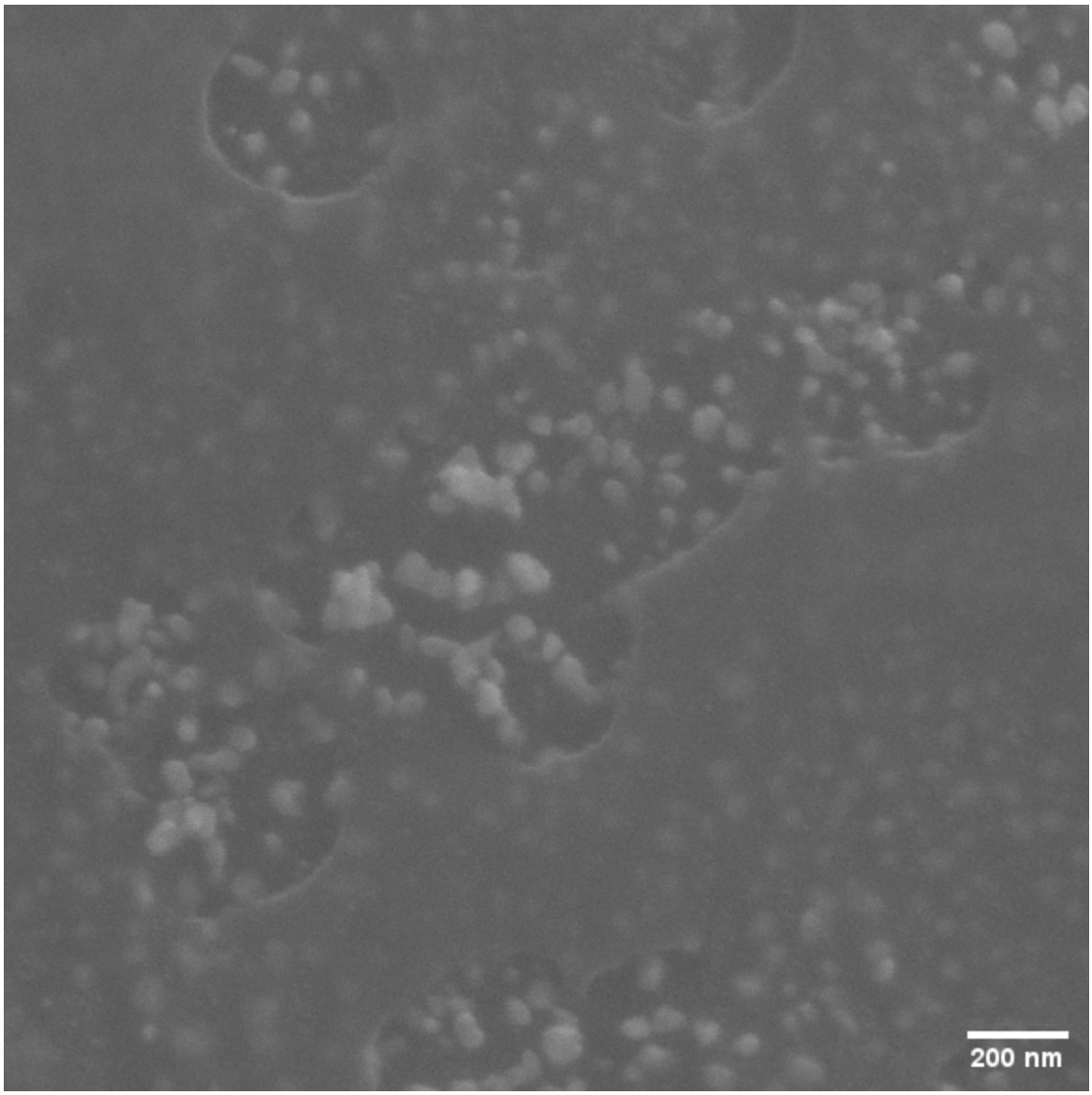

Figure 21: Sample grown at 550 °C for 30 minutes at gas ratio 1:40. Image taken from a top view at 30kx magnification.